12-19-2017

Biomechanical Tolerance of Whole Lumbar Spines in Straightened Posture Subjected to Axial Acceleration

Brian D. Stemper
Medical College of Wisconsin

Sajal Chirvi
Medical College of Wisconsin

Ninh Doan
Medical College of Wisconsin

Jamie L. Baisden
Medical College of Wisconsin

Dennis J. Maiman
Medical College of Wisconsin

See next page for additional authors

Accepted version. *Journal of Orthopaedic Research*, Vol. 36, No. 6 (December 19, 2017): 1747-1756. DOI.

Journal of Orthopaedic Research, Vol. 36, No. 6 (December, 2017): 1747-1756. DOI.

Biomechanical Tolerance of Whole Lumbar Spines in Straightened Posture Subjected to Axial Acceleration

Brian D. Stemper
Department of Neurosurgery, Medical College of Wisconsin, Milwaukee, WI
Department of Biomedical Engineering, Marquette University and Medical College of Wisconsin, Milwaukee, WI
Neuroscience Research, Clement J. Zablocki Veterns Affairs Medical Center, Milwaukee, WI
Sajal Chirvi
Department of Neurosurgery, Medical College of Wisconsin, Milwaukee, WI
Neuroscience Research, Clement J. Zablocki Veterans Affairs Medical Center, Milwaukee, WI
Ninh Doan
Department of Neurosurgery, Medical College of Wisconsin. Milwaukee, WI
Neuroscience Research, Clement J. Zablocki Veterans Affairs Medical Center, Milwaukee, WI
Jamie L. Baisden
Department of Neurosurgery, Medical College of Wisconsin, Milwaukee, WI
Neuroscience Research, Clement J. Zablocki Veterans Affairs Medical Center, Milwaukee, WI

Dennis J. Maiman
Department of Neurosurgery, Medical College of Wisconsin, Milwaukee, WI
Neuroscience Research, Clement J. Zablocki Veterans Affairs Medical Center, Milwaukee, WI
William H. Curry
Department of Neurosurgery, Medical College of Wisconsin, Milwaukee, WI
Neuroscience Research, Clement J. Zablocki Veterans Affairs Medical Center, Milwaukee, WI
Narayan Yoganandan
Department of Neurosurgery, Medical College of Wisconsin, Milwaukee, WI
Neuroscience Research, Clement J. Zablocki Veterans Affairs Medical Center, Milwaukee, WI
Frank A. Pintar
Department of Neurosurgery, Medical College of Wisconsin, Milwaukee, WI
Department of Biomedical Engineering, Marquette University and Medical College of Wisconsin, Milwaukee, WI
Neuroscience Research, Clement J. Zablocki Veterans Affairs Medical Center, Milwaukee, WI
Glenn Paskoff
Aircraft Division, Naval Air Warfare Center, Patuxent River, MD
Barry S. Shender
Aircraft Division, Naval Air Warfare Center, Patuxent River, MD

ABSTRACT

Quantification of biomechanical tolerance is necessary for injury prediction and protection of vehicular occupants. This study experimentally quantified lumbar spine axial tolerance during accelerative environments simulating a variety of military and civilian scenarios. Intact human lumbar spines (T12-L5) were dynamically loaded using a custom-built drop tower. Twenty-three specimens were tested at sub-failure and failure levels consisting of peak axial forces between 2.6 and 7.9 kN and corresponding peak accelerations between 7 and 57 g. Military aircraft ejection and helicopter crashes fall within these high axial acceleration ranges. Testing was stopped following injury detection. Both peak force and acceleration were significant ($p < 0.0001$) injury predictors. Injury probability curves using parametric survival analysis were created for peak acceleration and peak force. Fifty-percent probability of injury (95%CI) for force and acceleration were 4.5 (3.9–5.2 kN), and 16 (13–19 g). A majority of injuries affected the L1 spinal level. Peak axial forces and accelerations were greater for specimens that sustained multiple injuries or injuries at L2–L5 spinal levels. In general, force-based tolerance was consistent with previous shorter-segment lumbar spine testing (3–5 vertebrae), although studies incorporating isolated vertebral bodies reported higher tolerance attributable to a different injury mechanism involving structural failure of the cortical shell. This study identified novel outcomes with regard to injury patterns, wherein more violent exposures produced more injuries in the caudal lumbar spine. This caudal migration was likely attributable to increased injury tolerance at lower lumbar spinal levels and a faster inertial mass recruitment process for high rate load application.

Lumbar spine fractures occur in military environments.[1, 2] falls,[3] and vehicle crashes.[4, 5] Each scenario involves pelvis acceleration/deceleration contributing to compressive loads as forces transmitted through the pelvis compress the lumbar spine against the torso mass. Spinal motions lead to tissue deformation and injury occurs when local deformations exceed injury tolerance.[6-9] Non-physiologic compressive loads on the lumbar spine can injure vertebral bodies,[10-13] endplates,[12, 14] intervertebral discs,[15, 16] and posterior elements depending on segmental/spinal orientation[14, 17] and loading rate.[12, 13] Bony fractures can be acutely devastating, with immediate instability and possible fragmentation that can interact with neural tissues, producing significant neurological consequences.

Characteristics of lumbar spine injuries are modulated by the loading environment, including acceleration, applied force vector, and spinal alignment. While the science of injury biomechanics has defined specific mechanisms for different injury types (i.e., burst vs. compression vs. chance),[8] factors influencing the pattern of spinal injuries, including the number and location, have not been well defined. An example of loading conditions affecting injury outcome lies in the disparity of injury patterns between military and civilian environments.[18, 19] The distribution of lumbar spine injuries in modern soldiers demonstrated nearly 60% of thoraco–umbar fractures (T12-L5) affected the lower lumbar spine. However, lower spine injuries account for only 1% of spinal injuries in civilians.[2] Other studies supported this by demonstrating 53% of 266 spinal fractures attributed to underbody blast affected T12-L5 levels.[20] Caudal injury migration may be attributable to severe loading conditions in military personnel during aircraft ejections, helicopter crashes, or underbody blasts.[21] Vertical accelerations of 18 g with 250 g/s were established as the upper limit during the catapult phase of aviator seat egress in the Advanced Concept Ejection Seat (ACES). Helicopter crashes can be even more severe, although crash dynamics are complex with loading dependent upon altitude, airspeed, impact topography, seating type, and vehicle orientation.[22] Dynamics of underbody blast, studied to a lesser degree, may produce floor accelerations of 100–300 g over a 2.5 ms rise.[23, 24] Injury risk quantification using extrinsic parameters (e.g., acceleration) can assist in development of protection systems to attenuate/mitigate risks during occupant exposure.

If injury onset and pattern are influenced by loading characteristics, then those conditions can be used to predict injury onset and type. The Dynamic Response Index (DRI), used to quantify lumbar spine injury risk during vertical accelerations,[25] describes injury probability in terms of maximum spinal compression.[25, 26] However, DRI does not account for occupant age and sex, which can influence injury biomechanics,[27-29] and does not incorporate axial force or acceleration. Peak force is a common intrinsic metric for prediction of spinal injury under axial loads that is sensitive to occupant and environmental factors.[11-13, 27, 30] Additionally, clinical studies imply a role of acceleration in modulating injury patterns during vertical acceleration.

Considerable experimental effort was dedicated toward understanding lumbar spine injury tolerance and fracture mechanisms. However, most studies used isolated vertebrae,[12, 13, 31] short-segment models,[32, 33] or experiments that did not replicate the acceleration-induced mechanism of traumatic fractures in the field.[34, 35] Isolated vertebral body studies do not incorporate interaction of bony and soft tissues. Short segment models more effectively recreate this interaction and are valuable to define force-based tolerance, but are unable to demonstrate differing injury patterns and locations. Incorporation of weight-drop or electrohydraulic systems provides repeatable loading conditions, but

does not replicate the inertial-based loading scenario experienced during axial deceleration. This study had two objectives. The first objective was to quantify lumbar spine bony injury tolerance under vertical accelerative loading. The second objective was to quantify factors affecting injury outcomes including loading rate, peak force, age, and sex. These objectives were accomplished by incorporating whole lumbar columns and an experimental model that replicates the loading scenario associated with falls and motor vehicle events.[36]

METHODS

This manuscript describes an analytical study with Level of Evidence II. The study protocol was approved by the Research and Development Committee and all relevant subcommittees at the Zablocki Veterans Affairs Medical Center in Milwaukee, WI. Twenty-three human lumbar spines (T12-L5) were incorporated in the study. Pre-test CT scans were obtained of each specimen. The condition of the intervertebral disc and joint space, as well as the presence of bony osteophytes was graded at each spinal level according to a previously defined grading scale.[37] Specimens with excessive disc height loss, bridging osteophytes, or inconsistent alignment were not included in the study. Specimen demographics are provided in Table 1.

Table 1. Specimen-by-Specimen Biomechanical Data for Tests Producing Injury, Along With Injury Characteristics

Test ID	Age	Sex	Rate of Onset (g/s)	Force (kN)	Acceleration (g)	Injured Level	Fracture Classification	# Tests
1	18	F	221	5.6	19	L1	Endplate	5
						L2	Anterior Compression	
7	38	F	122	4.4	11	L1	Anterior Compression	1
						L2	Compression	
9	44	M	317	4.8	23	L1	Anterior Compression	1
						L1	Burst	
10	45	M	1,044	5.8	22	L4	Anterior Compression	6
11	45	F	289	3.8	23	L1	Anterior Compression	1
12	49	M	2,398	5.1	55	L3	Bilateral Pars	6
						L5	Burst, Bilateral Facet	
13	49	F	266	6.3	20	L5	Endplate	1
						L2	Anterior Compression	
14	50	F	2,083	7.9	57	L3	Burst, Bilateral Facet	3
15	50	F	195	3.8	20	L1	Burst	1
16	52	M	205	4.5	17	L1	Anterior Compression	2
17	54	M	289	5.8	17	L1	Anterior Compression	2
18	54	M	1,079	6.5	38	L1	Anterior Compression	1
						L2	Chance	

Test ID	Age	Sex	Rate of Onset (g/s)	Force (kN)	Acceleration (g)	Injured Level	Fracture Classification	# Tests
						L3	Bilateral Facet	
19	55	M	608	7.4	34	L1	Burst, Chance	1
20	55	F	433	4.5	21	L1	Anterior Compression	1
21	58	F	670	5.3	40	L1	Burst, Chance	1
						L2	Anterior Compression	
22	58	M	476	5.9	32	L1	Burst	1
23	63	F	224	6.8	20	L4	Anterior Compression	4
						L5	Facet	
Mean (Std Dev)			642 ± 665	5.5 ± 1.2	28 ± 13			

Maximum rate of onset (g/s) along with peak force and acceleration are presented. Spinal levels that sustained bony fracture and the fracture classification are also presented. Additionally, the total number of dynamic tests up to and including the injury-producing test is shown.

Preparation of each specimen for dynamic testing was conducted according to the following steps. Cranial (T12) and caudal (L5) vertebrae were mounted in polymethylmethacrylate (PMMA) to facilitate attachment to the experimental apparatus. Natural lordotic curvature for each specimen was not altered during this procedure and the L2–L3 intervertebral disc level was maintained close to horizontal in the global coordinate system for the sake of consistency between specimens. Although the intent was to place the L2–L3 disc horizontal, the authors acknowledge that the disc might not have been completely horizontal during the process of pouring the PMMA as this was conducted under a fume hood which precluded in situ imaging of the specimen prior to the pour. The intervertebral disc level was defined as a line through the anterior and posterior mid-heights of the L2–L3 intervertebral disc, which represented the mid-point of the exposed L1 through L4 vertebrae. Specimens were wrapped in saline-soaked gauze during the fixation procedure to prevent dehydration.

The experimental apparatus consisted of two decoupled horizontal platforms attached through low friction precision linear steel bearings to a vertically oriented 7.6-m monorail (Figure 1).[36] The caudal fixation of the specimen was attached to the lower platform through a load cell. A 32-kg mass was added to the upper platform to simulate static torso mass for a 50th percentile male.[38] Redundant linear accelerometers were attached to the lower platforms to measure vertical acceleration of the platform/specimen base.

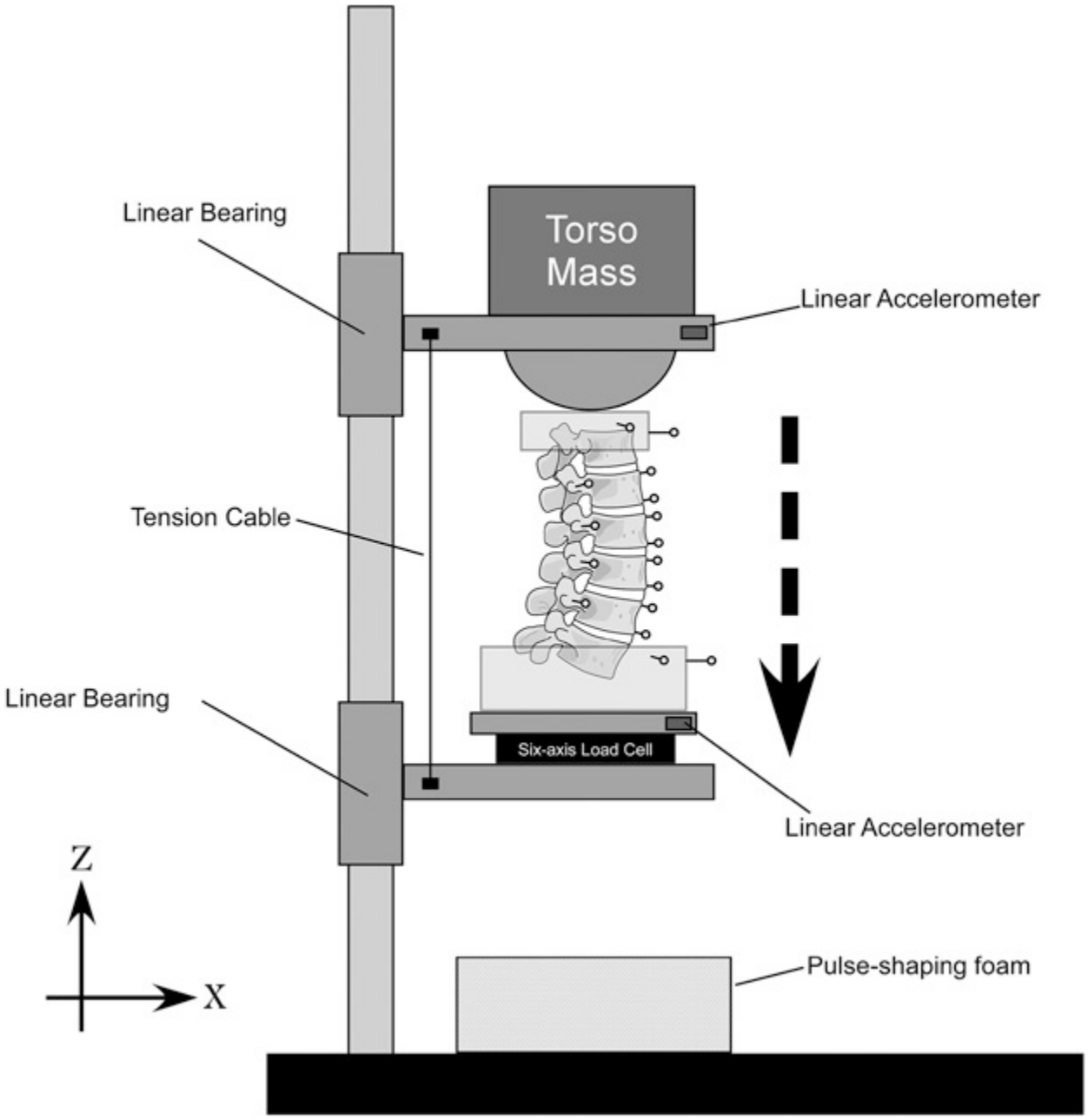

Figure 1 Vertical accelerator test setup to simulate high rate loading of the specimen.

Lateral X-rays were obtained of each specimen to confirm soft tissue integrity through an analysis of bony alignment/orientation at each spinal level. A pre-test qualitative assessment of specimen integrity and bending stiffness was then performed. Specimens were then flexed to 5 Nm by hand while minimizing off-axis bending moments using the data acquisition real-time mode. Orientation of the cranial fixation relative to the caudal fixation in the neutral and pre-flexed positions was used to determine forward rotation during the 5-Nm static preflexion, with flexion bending stiffness quantified as the 5-Nm applied load divided by the total rotation. These procedures were also repeated after each

dynamic test to qualitatively assess soft tissue injury as a remarkable change in segmental alignment/orientation or flexion bending stiffness from pre-test baseline assessments.

Specimens were prepared for dynamic testing following the integrity assessments described above, and prior to raising the specimens to the desired drop height. Preparation consisted of pre-flexion through the application of a 5-Nm flexion moment while minimizing off-axis loads. Cobb angles were measured prior to and following the 5-Nm flexion procedure. This was done to align the spine along its stiffest axis.[39] This orientation was maintained by placing the upper platform in contact with the cranial fixation at a location 3.0–3.5 cm anterior to the L2–L3 PLL. A cable was then attached between the platforms to prevent recoil of the specimen prior to the test and increased vertical displacement or bouncing during the dynamic test, while allowing the upper platform to decrease the vertical distance from the lower platform during deceleration, thus inertially compressing the lumbar spine specimen. Lateral and anterior–posterior X-rays were obtained with specimens in pre-test orientation.

Dynamic testing was initiated by raising the entire setup to the specific drop height and holding it in place using a high-power magnet. Removal of power from the magnet allowed gravity to accelerate the specimen to the base of the tower. Pulse-shaping foam (30 × 45 × 65 cm) was located at the drop tower base to provide a more realistic acceleration pulse. Foam characteristics were previously described.[36] As the lower platform was decelerated, the decoupled upper platform inertially loaded the cranial aspect of the specimen. Axial force and vertical accelerations were recorded at 20 kHz using a digital data acquisition system (Diversified Technical Systems, Inc., Seal Beach, CA).

Each specimen was exposed to one or more dynamic tests until injury was detected. Subsequent dynamic tests were from incremental drop heights for more severe loading exposures. This test procedure was incorporated previously in our laboratory to maximize specimen use as it permits development of non-failure and injury corridors using contributions from the same specimen.[40] Lateral X-rays were obtained following each test and compared to pre-test X-rays to identify bony fracture, or notable changes in spinal alignment or intervertebral disc heights. If X-ray images did not reveal bony injury, specimen palpation at each spinal level[41, 42] and flexion stiffness assessments described previously were used to identify the presence of laxity that was indicative of endplate or soft tissue injury. A clinical member of our team participated in the assessment of pre- and post-test X-ray images, as well as specimen palpations. Testing was stopped when injury (bony or soft tissue) was detected and post-test CT scans were obtained. X-ray and CT images were used to classify bony injuries based on the affected spinal level and type of fracture.[8] Soft tissue injuries were not a focus of this study and, therefore, any test producing soft tissue injury was not included in the analysis.

Data and Statistical Analysis

Lower platform accelerations and inertially compensated axial forces were used to develop injury risk curves using survival analysis with Weibull distribution.[43] Data from each specimen was categorized as either left, right, or interval censored. Data were treated as right censored for specimens that did not sustain bony injury. For specimens that sustained soft tissue injury, the test that yielded maximum axial force and acceleration prior to subfailure injury was incorporated as a non-injury test and the test producing soft tissue injury was not included. Data were treated as left censored for specimens that

sustained bony injury during the first test. Data were treated as interval sensored for specimens that underwent one or more subinjury tests prior to a test resulting in bony fracture. For this case, the subinjury test that yielded maximum axial force and acceleration was used for survival analysis and interval paired with the failure test.

Pairwise comparisons were also conducted between different groups to identify possible factors associated with changes in injury onset or patterns. Single factor Analysis of Variance (ANOVA) was used to identify significant differences ($p < 0.05$) in peak force and acceleration based on sex, between specimens that sustained one versus multiple fractured vertebrae, and between specimens that sustained fracture at L1 only versus any other level. Linear regression analysis was used to identify statistically significant correlations ($p < 0.05$) between specimen donor age and peak force or acceleration. Single factor ANOVA was also used to identify significant differences ($p < 0.05$) in peak force and acceleration between specimens that sustained bony fracture during the first test and specimens that were exposed to multiple dynamic tests.

RESULTS

The 23 specimens included in this study were subjected to a total of 38 tests. Pre-test grading of specimen degeneration revealed that a majority of specimens had no degenerative changes of the intervertebral disc or joint space, and did not have bony osteophytes. Eight specimens had at least one intervertebral disc level with mild degenerative changes and two specimens had one intervertebral disc level with moderate degenerative changes. One specimen had a single level with mild joint space narrowing and five specimens had a two levels with mild or moderate joint space narrowing. Five specimens had between one and three vertebrae with small osteophytes and two specimens had two vertebrae with small or medium sized osteophytes.

Preflexion of the specimens decreased the Cobb angle by an average of 12.8 ± 7.3° to a final Cobb angle of 22.2 ± 12.5°. Seventeen specimens sustained bony injury. Ten specimens were left-censored and the remaining seven specimens were interval-censored. Six tests producing only soft tissue injury were excluded and the prior high acceleration test for that specimen was included as right censored data. During bony injury-producing tests, acceleration rate of onset varied between 122 and 2,398 g/s, peak force varied between 3.8 and 7.9 kN, and peak acceleration varied between 11 and 57 g's (Table 1).

Injury Probability Curves

Peak force and acceleration were significant predictors of injury ($p < 0.0001$). Survival analysis demonstrated increasing risk for greater axial force and acceleration (Figs. 2 and 3). The force and acceleration with 95%CI at 10%, 50%, and 95% risk are presented in Table 2. The Normalized Confidence Interval Size (NCIS) for a selected probability, defined as 95% confidence interval width divided by mean value of the injury predictor at same selected probability, was used to measure tightness of fit.[43] The lower fraction indicates a tighter fit to the mean risk curve. The NCIS for force at

10%, 50%, and 95% injury probability risk is presented in Table 2. Risk curves for peak axial force and acceleration were not significantly dependent on age and sex ($p > 0.05$).

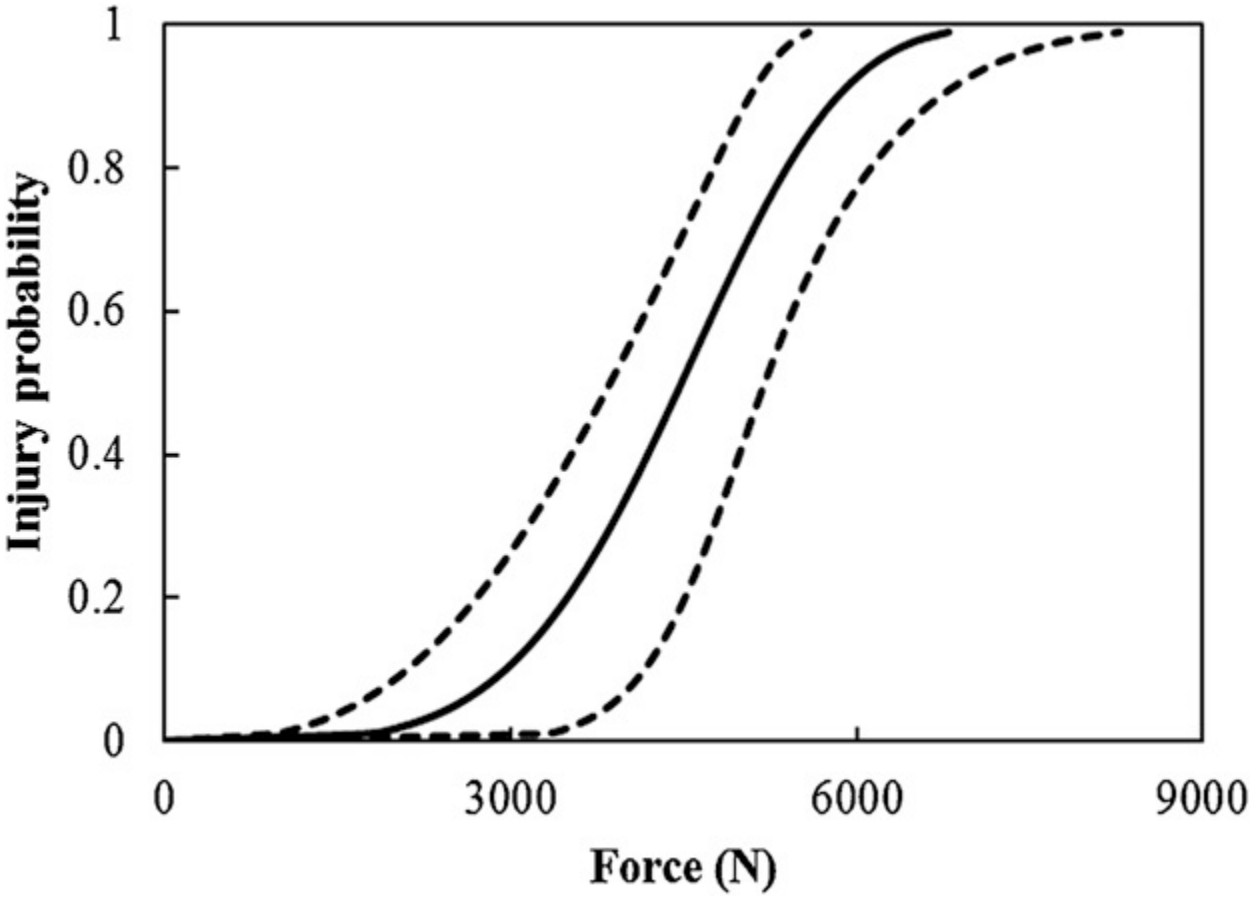

Figure 2 Injury probability curve using survival analysis for peak force. The plot shows the mean curve and 95% confidence intervals.

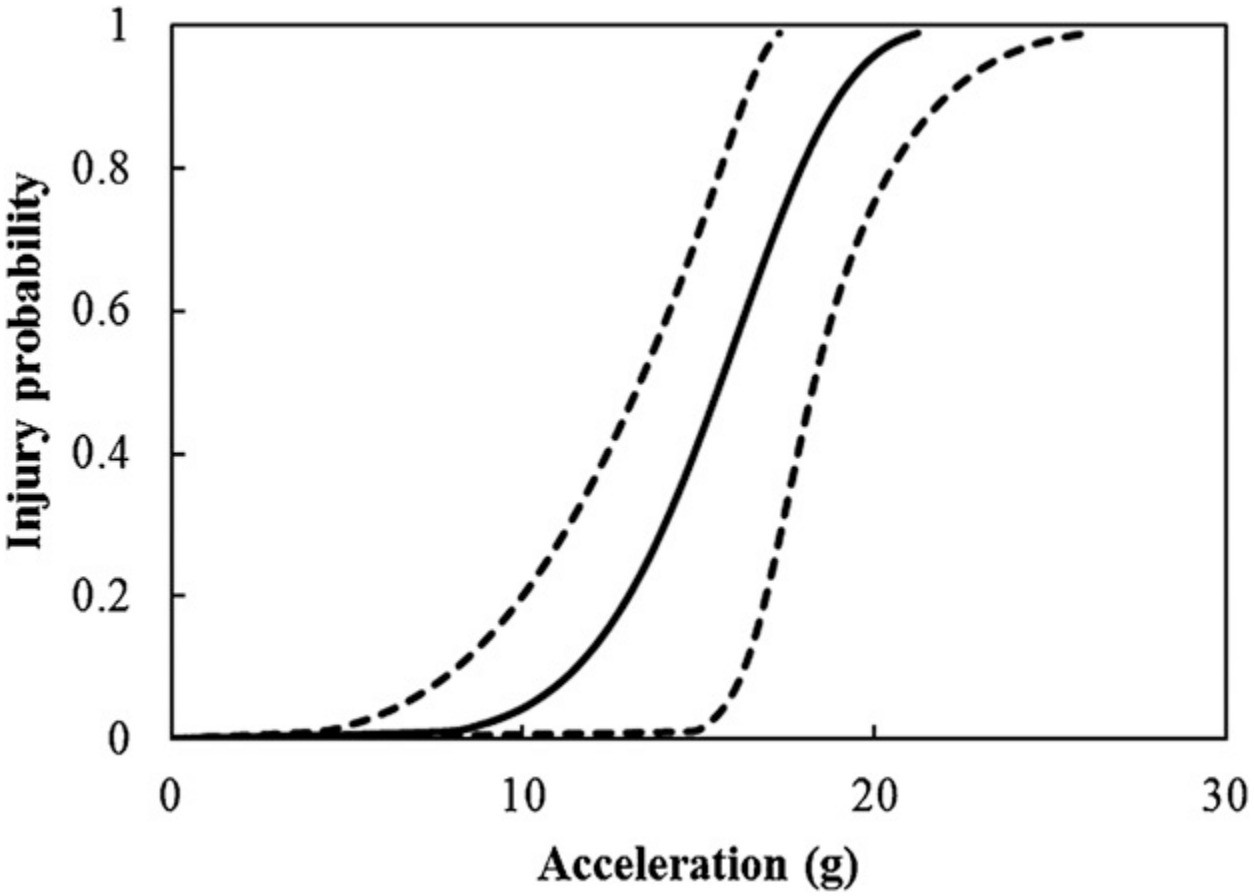

Figure 3 Injury probability curve using survival analysis for acceleration. The figure shows the mean curve and 95% confidence intervals (CI).

Table 2. Lumbar Spine Injury Risks Based on Compressive Force and Acceleration, With 95% Confidence Interval Presented in Parentheses

	10% Risk	**50% Risk**	**95% Risk**
Force (kN)	3.0 (2.1–4.2)	4.5 (3.9–5.2)	6.2 (5.3–7.3)
Acceleration (g)	12 (8–17)	16 (13–19)	20 (17–23)
NCIS, force	0.70	0.30	0.32
NCIS, acceleration	0.71	0.32	0.34

Normalized Confidence Intervals Sizes (NCIS) for force and acceleration are also presented.

Injury Documentation

Twenty-six fractures were identified in the seventeen specimens. Fracture distribution included 13 fractures at L1, five at L2, three at L3, two at L4, and three at L5. Representative CT scans of each fracture type are presented in Figure 4. Seven specimens had fractures at L1 only (Group (1), and ten had fractures at multiple levels or levels L1–L5 (Group (2). Peak force and acceleration were 15.1% and

25.8% greater in Group 2 specimens (Figs. 5 and 6). The effect size was greater for force (Cohen's d: 0.80) than acceleration (Cohen's d: 0.63). These effect sizes were greatest of all groupwise comparisons. However, peak force and acceleration were not significantly different between groups.

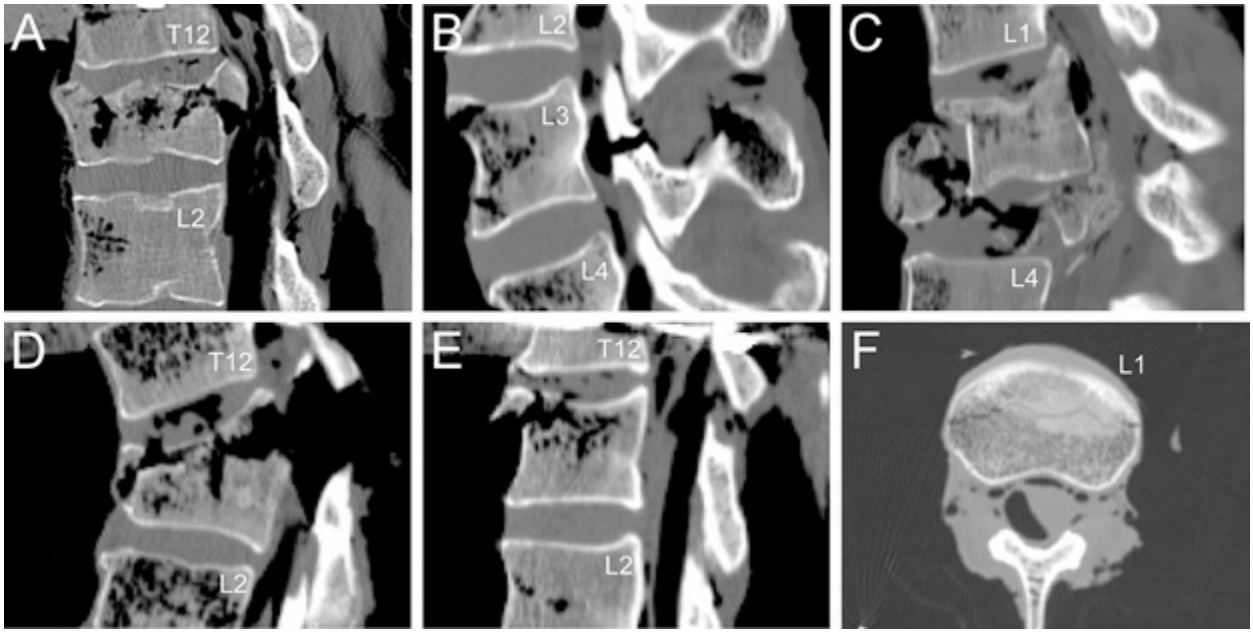

Figure 4 Images depicting fractures sustained by whole-column lumbar spine specimens in this study. (A) Burst fracture affecting the L1 vertebral body. (B) Fracture of the pars interarticularis affecting the L3 vertebra. (C) Burst fracture affecting the L3 vertebral body and anterior compression fracture affecting the L2 vertebral body. (D) Chance fracture affecting the L1 vertebra. (E) Anterior compression fracture affecting the L1 vertebral body. (F) Endplate fracture affecting the superior endplate of the L1 vertebral body.

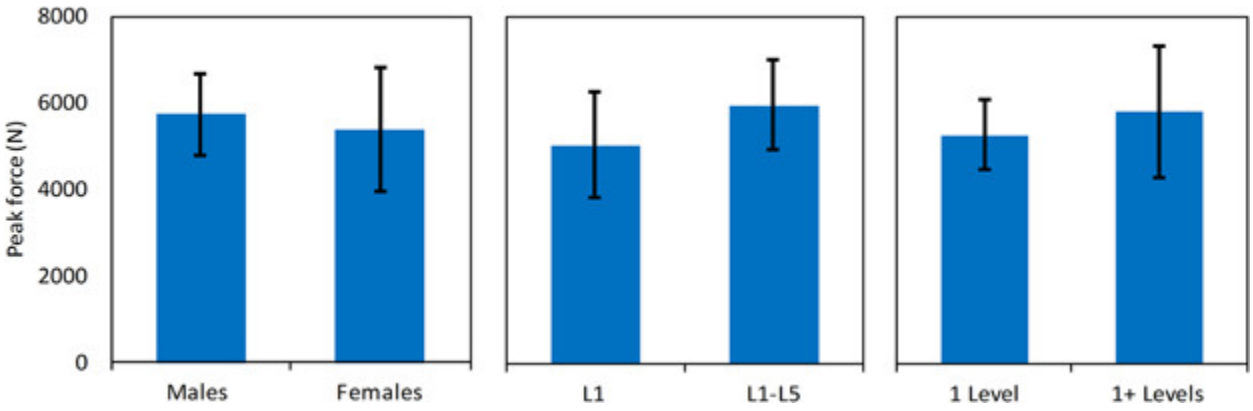

Figure 5 Peak force was not significantly different ($p > 0.05$) based on sex (left; Cohen's d: 0.28), for tests producing injury at L1 only versus other levels (middle; Cohen's d: 0.80), or for tests producing injuries at only one versus multiple levels (right; Cohen's d: 0.69).

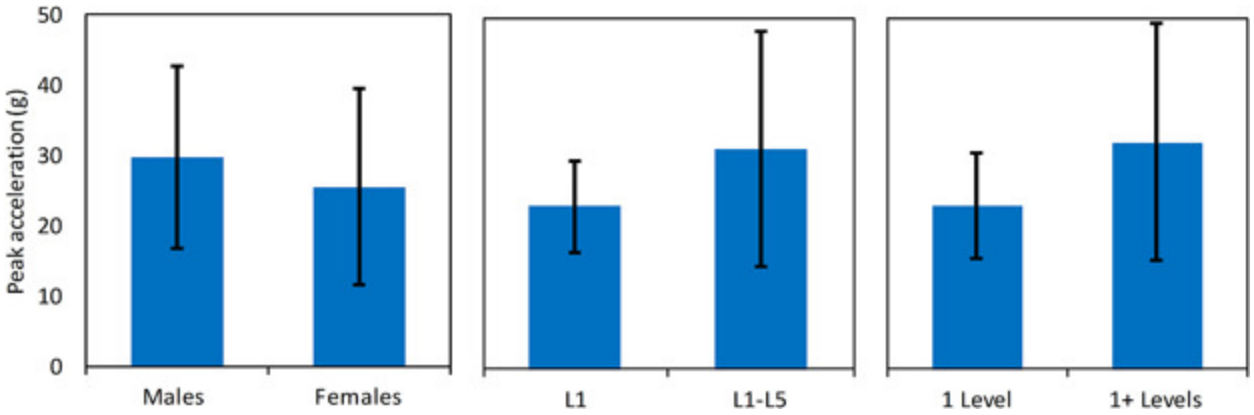

Figure 6 Peak acceleration was not significantly different ($p > 0.05$) based on sex (left; Cohen's d: 0.31), for tests producing injury at L1 only versus other levels (middle; Cohen's d: 0.63), or for tests producing injuries at only one versus multiple levels (right; Cohen's d: 0.57).

Mean peak axial force was 9.3% greater for tests that produced multiple fractures compared to those that produced one fracture (Cohen's d: 0.69). Tests resulting in multiple fractures had 28% greater peak acceleration (Cohen's d: 0.57). However, peak force and acceleration were not significantly different ($p > 0.05$) between the two groups. Sex differences resulted in increased peak force (6%) and acceleration (17%) in male specimens, with smaller effect sizes (Cohen's d: 0.28 for force and 0.31 for acceleration). Those differences were not statistically significant. Similarly, linear regression analysis indicated that there were no significant correlations between age and peak force or acceleration. Finally, there were no significant differences between specimens that sustained injury during the first test and specimens that were exposed to multiple dynamic tests.

DISCUSSION

The objectives of this study were to quantify lumbar spine injury tolerance during axial acceleration and identify factors affecting injury risk. Peak axial force (intrinsic) and peak vertical acceleration (extrinsic) were significant predictors of injury onset. The unique experimental model precludes comparison of acceleration-based findings, although a number of experimental studies quantified lumbar spine injury tolerance in terms of compressive force. Those studies primarily incorporated three-vertebra specimens, with the middle vertebra exposed to trauma[12, 32, 33, 44, 45] or isolated vertebral bodies.[12, 13] One study incorporating lumbar columns (T12-L5) reported fractures at the level of fixation (T12), although tolerance was in line with present results.[34] Dynamic experimental studies incorporating isolated vertebral bodies and short segments typically reported fracture forces that were greater than this study (5,542 ± 1,186 N) (Table 3). For vertebral bodies, this discrepancy likely arises from the fracture mechanism, which involves structural failure of the cortical shell. Compressive fracture in multi-level specimens involves endplate failure associated with compressive loads transmitted through the nucleus. Compressive tolerance of the endplate is lower than that of the cortical shell[14] because of its perpendicular orientation relative to applied loads and decreased thickness. Accordingly, peak compressive force for short segment models was only 9% greater than present findings. Smaller differences between fracture tolerance outlined in the current study from prior studies incorporating short segment models are more likely attributable to loading rate than

segment length, given the consistency in fracture mechanism between long and short column models. Prior studies incorporating shorter segments generally employed weight drop models and electrohydraulic piston compressions at rates that exceeded the local compression rates for dynamic whole-column tests in this study.[13, 36]

Table 3. Summary of Dynamic Experimental Studies and Reported Injury Tolerance Values

First Author	Year	Model	Exposed Level	Peak Force
Ochia	2003	Vertebral body	L4, L5	9.7 ± 2.1 kN
Stemper	2015	Vertebral body	L2–L4	9.0 ± 2.4 kN (lower rate, females) 10.8 ± 3.1 kN (higher rate, females) 8.1 ± 2.3 kN (lower rate, males) 8.9 ± 2.1 kN (higher rate, males)
Willen	1984	3-vertebra	L1	6.0–10.0 kN
Shono	1994	3-vertebra	L1	7.2 kN
Panjabi	1995	3-vertebra	T12, L1	6.7 ± 2.0 kN(neutral) 6.2 ± 2.3 kN (pre-flexed)
Kifune	1995	3-vertebra	T12	5.3–6.8 kN
Langrana	2002	3-vertebra	L1	5.8 ± 1.8 kN
Ochia	2002	3-vertebra	Not specified	4.2 ± 1.7 kN
Duma	2006	Whole column	L1–L5	5.0–5.9 kN
Present study		Whole column	L1–L5	5.5 ± 2 kN

Thoraco–lumbar injury risk curves were previously developed using this experimental model.[46] The 50% risk of fracture was 3.4 kN for thoracic spines and 3.7 kN for thoracic and lumbar spines. Lumbar spine data presented above revealed a 50% risk of injury shifted further to the right (4.5 kN). Acknowledging different statistical methodologies, this study is consistent with previously published thoraco–lumbar data. These data demonstrate a trend of increasing dynamic injury tolerance from thoracic to lumbar spines.

Injury Patterns

This study identified novel outcomes with regard to injury patterns by identifying trends of increasing force and acceleration for tests that produced injuries caudal to the L1 vertebra or at multiple spinal levels. Patterns with regard to acceleration have not been presented previously as a majority of studies incorporated fixed-base experimental models with the application of compressive loads through impact at the cranial aspect.[32, 34, 44, 45, 47, 48] Conversely, the unique experimental model incorporated in the current study recreated the cranially oriented load transfer associated with deceleration of the lumbar spine base while the simulated torso mass inertially loaded the specimen from the thoracolumbar junction.[36] Likewise, identification of differing injury patterns is also novel and permitted by the use of full-column lumbar specimens. A majority of prior work in this area has

included short segment models that focus injury at a single spinal level[32, 44, 45] and studies incorporating longer columns were not focused on outlining differences in injury pattern. Therefore, the current study provides useful biomechanical information with regard to injury outcomes that were clinically identified. A lack of statistically significant differences between groups (single vs. multiple injury or L1 vs. other levels) is likely more attributed to the somewhat limited sample size incorporated in this study.

A majority of fractures affected the cranial lumbar spine, with decreasing numbers at caudal levels. This outcome mirrors the injury distribution that occurs during high-rate vertical loading across a variety of military environments,[21] wherein a majority of injuries affected L1 with decreasing numbers caudally. Violent exposures produced more injuries in the caudal lumbar spine. Other studies demonstrated similar distributions.[2] An explanation for this acceleration-based injury pattern includes greater tolerance at caudal spinal levels,[10, 49] wherein greater accelerations produced greater and earlier onset of peak forces that exceed lower lumbar spine tolerance. This study demonstrated a non-significant trend of increasing peak force for injuries at caudal lumbar spinal levels. However, lumbar level-dependent injury tolerance was not universally reported.[13] Therefore, due to the modest increase in peak force and somewhat conflicting experimental evidence, the modulating factor for differing injury patterns in the lumbar spine may also be attributable to other mechanisms.

Another mechanism for caudal injury migration during high-rate loading involves the incorporation of rigid body armor in military personnel that lowers the lordotic/kyphotic transition zone from the thoracolumbar junction to the lower lumbar spine.[2] This explanation likely involves geometrical alignment and mass recruitment. Normal lumbar lordosis is not consistent from cranial to caudal extents. Rather, greater cephalad lordotic curvature gives way to a straighter cranial orientation.[50] This natural orientation biomechanically protects the lower lumbar spine, whereas the upper region is oriented according to the stiffest axis,[39] which explains why nearly 90% of spinal fractures affect the thoracolumbar junction.[2] However, preflexion of the lumbar spine in this study, which removed the lordotic curvature of the lower while maintaining the straighter upper lumbar spine, predisposed the entire lumbar spine to fracture along the stiffest axis.[17] This removed the cranial injury bias.

As lumbar spine straightening removed the injury bias from the thoracolumbar junction, injury location was then modulated by the rate of force application. Due to the relatively low contribution of the posterior elements in compression, the lumbar spine is essentially a series of rigid elements interconnected by viscoelastic discs with rate dependent properties. Axial forces act vertically against the torso reaction mass as the lumbar spine base is vertically accelerated/decelerated. However, the entire torso mass is not applied instantaneously due to the viscoelastic nature of the discs. Accordingly, increasing forces are transmitted up the lumbar spine until sufficient mass is recruited to exceed fracture tolerance. Rate-dependent properties manifest as increasing stiffness for higher compressive loading rates.[12, 13, 51] Therefore, the entire system stiffens at higher loading rates, mass is recruited more quickly, and fractures migrate caudally toward lower lumbar levels. However, this theory requires experimental or computational verification.

Identification of differences in lumbar spine injury patterns is relevant for military environments, wherein lower lumbar fractures are more common.[2] Military vehicles are different from civilian and

crash scenarios are more severe. Commonly encountered scenarios include aircraft ejection, helicopter crashes, and underbody blast exposure in ground-based vehicles. Each of those loading scenarios has a component of high rate vertical acceleration. Aircraft ejection accelerations of 18 G with 250 G/s were established as the upper limit for aviator egress in the Advanced Concept Ejection Seat (ACES). One study that analyzed 298 crashes occurring in military helicopters indicated that mean vertical change in velocity was 4.3–16.0 m/s for all crashes and 3.5–8.8 m/s for survivable crashes.[22] Seat pan accelerations measured during a full-scale military helicopter crash test with similar vertical velocity (11.6 m/s) were 40 and 33 g's occurring over approximately 15 ms for the pilot and co-pilot.[52] Mean accelerations from this study (28 g) fit within that range, with fractures occurring at accelerations between 11 and 57 g.

Sex-Based Differences

Specimen sex was not a statistically significant predictor for injury onset, although male specimens demonstrated greater force and acceleration at fracture. However, the lack of statistically significant differences is not conclusive evidence that this factor is not significant for the population as a whole. This study was not specifically designed to investigate this factor and loading conditions were not matched between sexes, which likely contributed to this negative result. Sex-based biomechanical differences were identified in a number of prior investigations. For example, lumbar vertebral bodies obtained from male donors had 19% greater ultimate force, although the difference did not attain statistical significance.[13] A larger study incorporating 700 volunteers identified significantly greater estimated vertebral strength in males.[53] Greater vertebral strength was attributed to increased cross-sectional area (CSA). That finding is consistent with our prior study, which reported greater ultimate stress in female specimens despite greater ultimate force in males.[13] We also reported a similar relationship for the physiologic response of thoracic disc segments.[54] Male specimens had greater compressive stiffness and CSA, but lower compressive modulus. Given consistent findings of larger and stronger vertebrae in males along with some indication of greater material modulus in females, these differences warrant further investigation.

Limitations

Experimental studies of spine biomechanics have often used follower loads to simulate the static compressive load on the lumbar spine due to the mass of the torso and static contraction of paraspinal muscles, which has been estimated to be as high as 500–1,000 N.[55-57] Follower loads orient compressive forces along the line of the lordotic curvature and were shown to add stability to the lumbar spine and increase the bending and shear stiffness.[58, 59] Other studies demonstrated that the compressive loading carrying capacity of the lumbar spine was increased to more physiologic levels when static forces were applied using follower loads.[58] However, follower loads were not incorporated in the current study for two primary reasons. Firstly, cable guides consisting of small screws attached to the lateral aspects of the vertebral bodies would likely not hold up to the large forces generated during these dynamic experiments and repeated pull-out of these screws would weaken the cortical shell and decrease compressive tolerance of the vertebral bodies. Secondly, suspension of the simulated torso mass using cables would likely pose a laboratory safety hazard as the experimental

apparatus was decelerated at rates exceeding 50 g. To account for this, the current study incorporated a protocol that involved application of the torso mass using a weighted decoupled platform in contact with the cranial aspect of the specimen. All specimens were also oriented with 5 Nm of flexion prior to dynamic testing to prevent buckling during dynamic load application and ensure that compressive loads were applied along the line of the lumbar spine. Cobb angles were decreased by an average of 12.8 ± 7.3°, which produced a straighter spine, acknowledging that the axial line may have been somewhat forward of the vertically applied load.

Another possible limitation of the current experimental protocol could be the use of repeated dynamic tests in some specimens, whereas other specimens were only exposed to a single test. The intent of this protocol was to maximum specimen use and our prior studies have not identified remarkable changes in specimen biomechanical response attributable to repetitive and incremental dynamic exposures.[40] Nonetheless, a relevant criticism is that multiple tests could weaken the biomechanical tolerance or alter other aspects of the biomechanical response. However, as shown in Table 1 and highlighted in the Results above, there was no significant difference in peak force or acceleration for specimens exposed to multiple dynamic tests versus specimens that sustained bony fracture during the initial exposure. Therefore, although not a comprehensive investigation, repeated incremental testing did not appear to remarkably alter specimen biomechanics or tolerance in this study.

CONCLUSION

This study quantified axial tolerance of intact lumbar spines using an acceleration-based experimental model. Axial force and peak acceleration were significant injury predictors. Lumbar spine injury risk curves were derived. Injured specimens were further categorized by affected spinal level with a majority affecting L1. Peak axial force and acceleration did not attain statistical significance for the level of injury, although the effect size for this comparison was the largest of all groupwise comparisons. Results contribute to the understanding of biomechanical tolerance and fracture pattern of lumbar spine injuries during dynamic axial loading.

AUTHORS' CONTRIBUTIONS

Dr. BDS contributed to all aspects of this manuscript including experimental design and analysis, injury identification and interpretation, and manuscript preparation and proofreading. Dr. SC was involved in experimental analysis and injury identification as well as manuscript preparation and proofreading. Dr. ND was involved in data analysis, injury identification and interpretation, and proofreading of the manuscript. Drs. JLB and DJM were involved in experimental design, injury identification and interpretation, and proofreading of the manuscript. Drs. FAP, NY, and BSS were involved in experimental design and data analysis, manuscript preparation, and proofreading. Mr. GP was involved in experimental design and data analysis, as well as proofreading of the manuscript. All authors have read and approved the final submitted manuscript.

References

1 Edwards M. 1996. Anthropometric measurements and ejection injuries. *Aviat Space Environ Med* 67:1144–1147.

2 Lehman RA Jr., Paik H, Eckel TT, et al. 2012. Low lumbar burst fractures: a unique fracture mechanism sustained in our current overseas conflicts. *Spine J* 12:784–790.

3 Richter D, Hahn MP, Ostermann PA, et al. 1996. Vertical deceleration injuries: a comparative study of the injury patterns of 101 patients after accidental and intentional high falls. *Injury* 27:655–659.

4 Muller CW, Otte D, Decker S, et al. 2014. Vertebral fractures in motor vehicle accidents—a medical and technical analysis of 33,015 injured front-seat occupants. *Accid Anal Prev* 66:15–19.

5 Pintar FA, Yoganandan N, Maiman DJ, et al. 2012. Thoracolumbar spine fractures in frontal impact crashes. *Ann Adv Automot Med* 56:277–283.

6 Aebi M. 2010. Classification of thoracolumbar fractures and dislocations. *Eur Spine J* 19:S2–S7.

7 Schmorl G, Junghanns H. 1971. The human spine in health and disease. New York, NY: Grune & Stratton, Inc.

8 Stemper BD, Pintar FA, Baisden JL. 2015. Lumbar spine injury biomechanics. In: Yoganandan N, Nahum AM, Melvin JW, editors. Accidental injury: biomechanics and prevention, 3rd ed. New York, NY: Springer Science + Business Media.

9 Denis F. 1984. Spinal instability as defined by the three-column spine concept in acute spinal trauma. *Clin Orthop Relat Res* 189:65–76.

10 Hansson T, Roos B, Nachemson A. 1980. The bone mineral content and ultimate compressive strength of lumbar vertebrae. *Spine (Phila Pa 1976)* 5:46–55.

11 Kazarian L, Graves GA. 1977. Compressive strength characteristics of the human vertebral centrum. *Spine (Phila Pa 1976)* 2:1–14.

12 Ochia RS, Tencer AF, Ching RP. 2003. Effect of loading rate on endplate and vertebral body strength in human lumbar vertebrae. *J Biomech* 36:1875–1881.

13 Stemper BD, Yoganandan N, Baisden JL, et al. 2015. Rate-dependent fracture characteristics of lumbar vertebral bodies. *J Mech Behav Biomed Mater* 41:271–279.

14 Curry WH, Pintar FA, Doan NB, et al. 2016. Lumbar spine endplate fractures: biomechanical evaluation and clinical considerations through experimental induction of injury. *J Orthop Res* 34:1084–1091.

15 Brinckmann P, Porter RW. 1994. A laboratory model of lumbar disc protrusion. Fissure and fragment. *Spine (Phila Pa 1976)* 19:228–235.

16 Adams MA, Hutton WC. 1982. Prolapsed intervertebral disc. a hyperflexion injury 1981 Volvo Award in Basic Science. *Spine (Phila Pa 1976)* 7:184–191.

17 Maiman DJ, Yoganandan N, Pintar FA. 2002. Preinjury cervical alignment affecting spinal trauma. *J Neurosurg* 97:57–62.

18 Belmont PJ Jr., Goodman GP, Zacchilli M, et al. 2010. Incidence and epidemiology of combat injuries sustained during “the surge” portion of operation Iraqi Freedom by a U. S. Army brigade combat team. *Trauma* 68:204–210.

19 Owens BD, Kragh JF Jr., Wenke JC, et al. 2008. Combat wounds in operation Iraqi freedom and operation enduring freedom. *J Trauma* 64:295–299.
20 Spurrier E, Singleton JA, Masouros S, et al. 2015. Blast injury in the spine: dynamic response index is not an appropriate model for predicting injury. *Clin Orthop Relat Res* 473:2929–2935.
21 Stemper BD, Yoganandan N, Paskoff GR, et al. 2011. Thoracolumbar spine trauma in military environments. *Minerva Ortopedica E Traumatologica* 62:397–412.
22 Shanahan DF, Shanahan MO. 1989. Kinematics of U.S. army helicopter crashes: 1979–85. *Aviat Space Environ Med* 60:112–121.
23 Wang J, Bird R, Swinton B, et al. 2001. Protection of lower limbs against floor impact in army vehicles experiencing landmine explosion. *J Battlefield Technol* 4:8–12.
24 Hirsch A. 1963. Man's response to shock motions, in Winter Annual Meeting of the American Society of Mechanical Engineers (ASME). Philadelphia, PA: American Society of Mechanical Engineers. p 63-WA-283.
25 DeStefano LA. 1972. Dynamic response index minimization for personnel escape systems. Phildelphia, PA: Frankford Arsenal.
26 Thyagarajan R, Ramalingam J, Kulkarni KB. 2014. Comparing the use of dynamic response index (DRI) and lumbar load as relevant spinal injury metrics. Warren, MI: U.S. Army Tank Automotive Research, Development and Engineering Center.
27 Pintar FA, Yoganandan N, Voo L. 1998. Effect of age and loading rate on human cervical spine injury threshold. *Spine (Phila Pa 1976)* 23:1957–1962.
28 Stemper BD, Pintar FA, Rao RD. 2011. The influence of morphology on cervical injury characteristics. *Spine (Phila Pa 1976)* 36:S180–S186.
29 Stemper BD, Hallman JJ, Pintar FA, Maiman DJ. 2013. Gender and aging: considerations for orthopaedics. In: Winkelstein BA, editor. Orthopaedic Biomechanics. Boca Raton, FL: CRC Press & Taylor and Francis Group.
30 Nightingale RW, McElhaney JH, Richardson WJ, et al. 1996. Dynamic responses of the head and cervical spien to axial impact loading. *J Biomech* 29:307–318.
31 Hansson T, Roos B. 1981. The relation between bone mineral content, experimental compression fractures, and disc degeneration in lumbar vertebrae. *Spine (Phila Pa 1976)* 6:147–153.
32 Langrana NA, Harten RR, Lin DC, et al. 2002. Acute thoracolumbar burst fractures: a new view of loading mechanisms. *Spine (Phila Pa 1976)* 27:498–508.
33 Panjabi MM, Kifune M, Wen L, et al. 1995. Dynamic canal encroachment during thoracolumbar burst fractures. *J Spinal Disord* 8:39–48.
34 Duma SM, Kemper AR, McNeely DM, et al. 2006. Biomechanical response of the lumbar spine in dynamic compression. *Biomed Sci Instrum* 42:476–481.
35 Mermelstein LE, McLain RF, Yerby SA. 1998. Reinforcement of thoracolumbar burst fractures with calcium phosphate cement. A biomechanical study. *Spine (Phila Pa 1976)* 23:664–670. discussion 670–671.
36 Stemper BD, Storvik SG, Yoganandan N, et al. 2011. A new PMHS model for lumbar spine injuries during vertical acceleration. *J Biomech Eng* 133:081002.

37 Lane NE, Nevitt MC, Genant HK, et al. 1993. Reliability of new indices of radiographic osteoarthritis of the hand and hip and lumbar disc degeneration. *J Rheumatol* 20:1911–1918.
38 Clauser CE, McConville JT, Young JW. 1969. Weight, volume, and center of mass of segments of the human body. Ohio: Wright-Patterson Air Force Base.
39 Liu YK, Dai QG. 1989. The second stiffest axis of a beam-column: implications for cervical spine trauma. *J Biomech Eng* 111:122–127.
40 Stemper BD, Yoganandan N, Pintar FA. 2003. Gender dependent cervical spine segmental kinematics during whiplash. *J Biomech* 36:1281–1289.
41 Stemper BD, Yoganandan N, Pintar FA, et al. 2011. The relationship between lower neck shear force and facet joint kinematics during automotive rear impacts. *Clin Anat* 24:319–326.
42 Crandall JR, Bose D, Forman J, et al. 2011. Human surrogates for injury biomechanics research. *Clin Anat* 24:362–371.
43 Yoganandan N, Pintar F, Banerjee A, et al. 2015. Hybrid III lower leg injury assessment reference curves under axial impacts using matched-pair tests. *Biomed Sci Instrum* 51:230–237.
44 Kifune M, Panjabi MM, Liu W, et al. 1997. Functional morphology of the spinal canal after endplate, wedge, and burst fractures. *J Spinal Disord* 10:457–466.
45 Willen J, Lindahl S, Irstam L, et al. 1984. The thoracolumbar crush fracture. An experimental study on instant axial dynamic loading: the resulting fracture type and its stability. *Spine (Phila Pa 1976)* 9:624–631.
46 Yoganandan N, Arun MW, Stemper BD, et al. 2013. Biomechanics of human thoracolumbar spinal column trauma from vertical impact loading. *Ann Adv Automot Med* 57:155–166.
47 Fredrickson BE, Edwards WT, Rauschning W, et al. 1992. Vertebral burst fractures: an experimental, morphologic, and radiographic study. *Spine (Phila Pa 1976)* 17:1012–1021.
48 Ochia RS, Ching RP. 2002. Internal pressure measurements during burst fracture formation in human lumbar vertebrae. *Spine (Phila Pa 1976)* 27:1160–1167.
49 Yoganandan N, Stemper BD, Baisden JL, et al. 2015. Effects of acceleration level on lumbar spine injuries in military populations. *Spine J* 15:1318–1324.
50 Dai LD. 2002. Low lumbar spinal fractures: management options. *Injury* 33:579–582.
51 Kemper AR, McNally C, Duma SM. 2007. The influence of strain rate on the compressive stiffness properties of human lumbar intervertebral discs. *Biomed Sci Instrum* 43:176–181.
52 Jackson KE, Fasanella EL, Boitnott R, et al. 2004. Occupant responses in a full-scale crash test of the Sikorsky ACAP helicopter. *J Am Helicopter Soc* 49:127–139.
53 Bouxsein ML, Melton LJ 3rd, Riggs BL, et al. 2006. Age- and sex-specific differences in the factor of risk for vertebral fracture: a population-based study using QCT. *J Bone Miner Res* 21:1475–1482.
54 Stemper BD, Board D, Yoganandan N, et al. 2010. Biomechanical properties of human thoracic spine disc segments. *J Craniovertebr Junction Spine* 1:18–22.
55 Nachemson A. 1966. The load on lumbar disks in different positions of the body. *Clin Orthop Relat Res* 45:107–122.
56 Wilke H, Neef P, Hinz B, et al. 2001. Intradiscal pressure together with anthropometric data?a data set for the validation of models. *Clin Biomech (Bristol, Avon)* 16:S111–S126.

57 Callaghan JP, McGill SM. 2001. Low back joint loading and kinematics during standing and unsupported sitting. *Ergonomics* 44:280–294.
58 Patwardhan AG, Havey RM, Meade KP, et al. 1999. A follower load increases the load-carrying capacity of the lumbar spine in compression. *Spine (Phila Pa 1976)* 24:1003–1009.
59 Janevic J, Ashton-Miller JA, Schultz AB. 1991. Large compressive preloads decrease lumbar motion segment flexibility. *J Orthop Res* 9:228–236.